

Phase engineering of squeezed states and controlled entangled number states of Bose-Einstein condensates in multiple wells

Khan W. Mahmud,¹ Mary Ann Leung,² and William P. Reinhardt^{1,2}

¹Department of Physics, University of Washington, Seattle, WA 98195-1560, USA

²Department of Chemistry, University of Washington, Seattle, WA 98195-1700, USA

We provide a scheme for the generation of entangled number states of Bose-Einstein condensates in multiple wells, and also provide a novel method for the creation of squeezed states without severe adiabatic constraints on barrier heights. The condensate ground state in a multiple well trap can be evolved, starting with specific initial phase difference between the neighboring wells, to a state with controllable entanglement. We propose a general formula for appropriate initial phase differences between the neighboring wells that is valid for any number of wells, even and odd.

Entanglement, a nonclassical correlation between two or more physical systems, lies at the heart of the profound difference between quantum mechanics and a local classical description of the world [1]. Apart from their discussions in the philosophical and foundational aspects of quantum mechanics [2], entangled states in recent years have become an essential resource for the emerging field of quantum information processing. Entangled states have been created with photons [3], four atoms [4], and most recently with many cold atoms in a Mott insulating state in an optical lattice [5]. Cold atoms in optical lattices have been a vibrant research area with several new observations such as the superfluid to Mott insulator transition [6] and number-squeezed states of Bose-Einstein condensate (BEC) [7]. Entangled and squeezed states hold promise in studies related to quantum measurement, the Heisenberg limited atom interferometry and quantum computing and quantum communication protocols [8]. While the consequence of entanglement for an Einstein-Podolsky-Rosen (EPR) pair is quantified in Bell's inequality [9], a more striking conflict between quantum mechanics and local realism is exhibited by three maximally entangled particles also known as the Greenberger-Horne-Zeilinger (GHZ) states [10]. GHZ state of N particles has the form

$$|\psi\rangle = \frac{1}{\sqrt{2}} (|1\rangle^N + |2\rangle^N) \quad (1)$$

where 1 and 2 are the basis states for a two state (spin $\frac{1}{2}$) system, and are written in the standard notation as $|j\rangle = |j\rangle_1 \dots |j\rangle_N$. In the occupation number basis, $|j\rangle^N$ and $|k\rangle^N$ respectively denote, $|N; 0\rangle$ and $|j; N\rangle$. The two-state model has been generalized to more than two spin components in Ref. [11]. The superposition of two macroscopically distinct states, rather than simply the internal degrees of freedom, each occupied by all N particles, has been discussed by Schrodinger in the famous cat parable [12]; partial realization of such states has been obtained with Josephson junction loops [13].

In this paper, we discuss the generation of macroscopic

entangled number states of a multiwell BEC of the form

$$|\psi\rangle = \frac{1}{\sqrt{M}} (|1\rangle^N + |2\rangle^N + \dots + |M\rangle^N) \quad (2)$$

where $1; 2; 3; \dots; M$ label the macroscopically and spatially distinct wells, $|j\rangle^N$ now denoting $|j; 0; \dots; N; \dots; 0\rangle$. We show that states approximating the extreme entangled states of Eq. (2) may be generated in a controlled fashion by time evolution of appropriately phase imprinted ground states of a multiwell BEC with periodic boundary conditions for $M = 3$ and 4 . We show that the choice of initial barrier heights, which determine the extent of ground state number squeezing, and the rate of barrier ramping can be used to control the extent of entanglement of the final states. We also show that fully fragmented states can be generated via natural time evolution from the ground state following certain initial phase offsets. The creation of such fragmented states through phase engineering and without the severe adiabatic constraints on the rate of barrier height change provides an alternative to the current experimental approaches [6, 7]. Finally, based on results obtained for two, three, and four well configurations, we conjecture a generalized formula, for M wells, for the phase offset between neighboring wells appropriate for the generation of number entangled states.

We approximate the physics of a BEC in a multiwell potential by the Bose-Hubbard model [14]. Thus

$$\hat{H} = \sum_j J (a_{i+1}^\dagger + a_{i+1}^\dagger a_i) + \sum_i \epsilon_i n_i + \frac{1}{2} U \sum_i n_i (n_i - 1) \quad (3)$$

where $n_i = a_i^\dagger a_i$ is the number operator, J is the nearest neighbor tunneling term, U is the on-site energy, and ϵ_i is the energy offset of the i th lattice. To simplify a theoretical study, we make a one parameter approximation of the tunneling and mean-field terms: $U = J = 1 = e$; and, for the symmetric wells explored here, $\epsilon_i = 0$. e is a dimensionless parameter that can be mapped onto the barrier height. This parameterization allows a simple

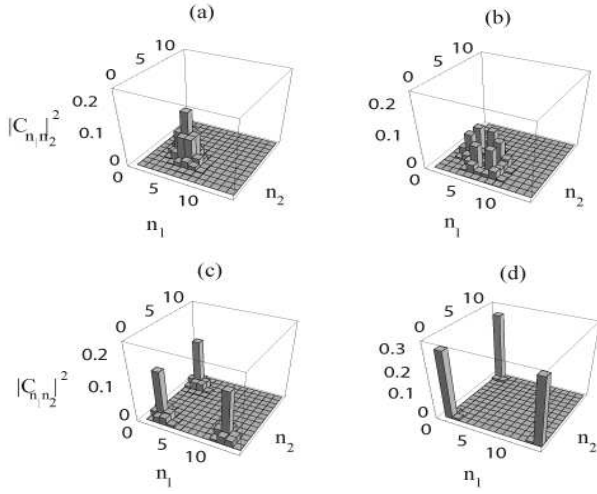


FIG. 1: Fock state coefficients for 12 particles in three wells: (a) the ground state, (b) 10th, (c) 76th and (d) 91st, the highest state. The ground state has a Gaussian shape, while higher lying states are entangled number states. n_1 and n_2 are the Fock state indices and the vertical axis shows probabilities. Points beyond the cross-diagonal are unphysical.

study of continuous change of barrier height through the variation of a single parameter α . For example, for a lattice made of red detuned laser with $\lambda = 985$ nm and for ^{23}Na , a barrier height $15E_R$ gives $U = 0.15E_R$ and $J = 0.07E_R$ [14] where $E_R = \frac{\hbar^2 k^2}{2m}$ is the recoil energy from absorption of a photon; these experimental parameters then correspond to $\alpha = 2.14$.

In order to gain insight into the types of stationary states possible for the multiwell Bose-Hubbard model, we first analyze the quantum mechanical properties of the simplest multiwell potential, $M = 3$, assuming three symmetric wells in a circular array [15]. The state vector is a superposition of all the number states

$$|j_i\rangle = \sum_{n_1, n_2=0}^N c_{n_1, n_2}^{(i)} |j_1; n_2; n_3\rangle \quad (4)$$

Here n_1, n_2 , and $n_3 = N - n_1 - n_2$ are the number of particles in each of the three wells. Fig. 1 shows the Fock space probabilities, $c_{n_1, n_2}^{(i)2}$, for representative stationary states for $N = 12$ and $\alpha = 0$ ($U=J = 1$). Our method of graphical representation is described in the figure caption. The ground state in Fig. 1 (a) is a broad Gaussian while the higher lying states, Figs. 1 (b)–(d), are number entangled states of increasing extremity corresponding to increasing numbers of particles simultaneously in all three wells, the highest of which in panel (d) is an extreme superposition state of the form $|j; 0; 0\rangle + |j; N; 0\rangle + |j; 0; N\rangle$. The number of non vanishing Fock state coefficients determines sharpness, and thus (d) is sharper than (c).

It is unlikely that such maximally entangled states can

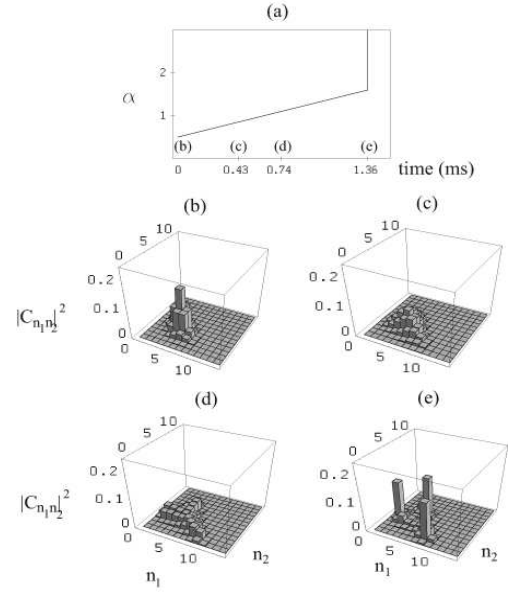


FIG. 2: Evolution to an entangled Fock space state: (a) barrier ramp showing the location of the following time evolved states: (b) initial state, (c) at 0.43 ms the Gaussian distribution broadens, (d) at 0.74 ms the distribution is ‘splitting’, (e) A three-peaked state is formed at 1.36 ms; a macroscopic superposition of definite number of particles simultaneously in all three wells.

be generated via a sequence of single particle excitations. They may however, be dynamically generated via phase engineering from the appropriate ground state. Writing phases on part of a condensate is experimentally feasible via interaction with a far off-resonance laser [16], and is assumed to be sudden with respect to the dynamics of the condensate [16]. Mathematically, this corresponds to multiplying the coefficients in an expansion of the type of Eq.(4) by $e^{in_i \phi}$, where $|j_1; n_2; \dots; n_i; \dots\rangle$ is the corresponding Fock state, and ϕ is the phase for particles in the i th well. Entangled state generation, obtained via integration of the (linear) time-dependent Schrödinger equation, is shown in Fig. 2, following phase imprinting of an initial phase difference of $\frac{2\pi}{3}$ between the neighboring wells, and a simultaneous linear ramping of the barrier as $\alpha = t$, as shown in Fig. 2 (a) (there is dimensionless). Panels 3 (b) shows the initial ground state; 3 (c) at time 0.43 ms, the distribution broadens; 3 (d) at 0.74 ms, in the process of splitting the state towards the three corners; and 3 (e) at 1.36 ms a sharp, although not extreme, entangled number state with its signature of three major non vanishing expansion coefficients. The times are given for a ^{87}Rb condensate, $\lambda = 840$ nm, $a_{sc} = 5.8$ nm, $J = 0.04E_R$ and taking $U = 0.04E_R$ as approximately constant for calculational purposes. When an appropriately entangled state is reached the barrier is suddenly raised to halt further evolution in n -space. For the parameter values

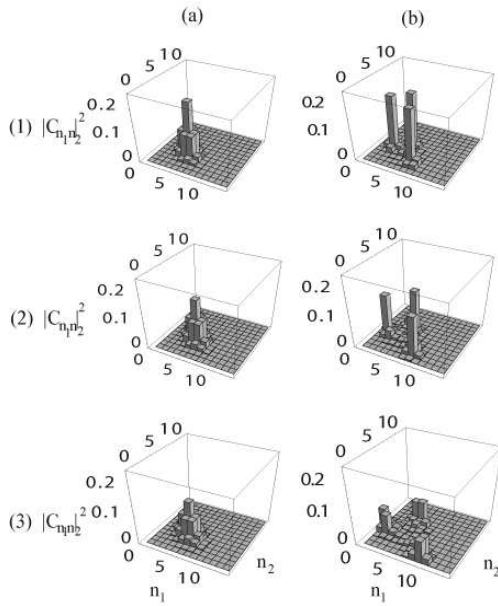


FIG. 3: Entangled states evolved from ground states with different initial squeezing. Row (1) shows the states with $\xi = 1.5 + t$: (a) initial ground state and (b) final state. Row (2) is for $\xi = 0.5 + t$ and (3) is for $\xi = t$. Column (b) gives the states at $t = 1.85$ ms, $t = 1.36$ ms, and $t = 0.99$ ms respectively. The initial squeezing of the ground state thus determines the extremity of the resulting entangled states.

used here, a simple time evolution without any change of barrier also produces an entangled state, however barrier ramping is used here to sharpen the resulting state. Control of the extremity of the states can be achieved by choice of the initial barrier height, controlling the initial squeezing of the ground state. This is demonstrated in Fig. 3, where different initial squeezing have been used for rows (1), (2) and (3). The columns show: (a) the ground state, and (b) the final state at the end of the barrier ramping. It is important to be able to tune to less extreme entangled states, as such states are more robust to loss and decoherence [17]. Phase imprinting with a phase difference of $\frac{4}{3}$ produces an equivalent state, with different phase space dynamics.

The physics of the creation of these entangled states can be understood in terms of the underlying classical phase space dynamics. Entangled state generation in a double well has been thoroughly analyzed in a semiclassical phase space picture [17]. In the semiclassical limit valid for large N , the operators \hat{a}_i can be approximated by the c-numbers $\sqrt{n_i} e^{i\phi_i}$, where n_i and ϕ_i are the number and phase of particles in the i th well. The double well dynamics is then described by the Hamiltonian of a nonrigid physical pendulum [18] with the number and phase differences (n, ϕ) between the wells as conjugate variables. This system has two fixed points – $(0, 0)$ and $(0, \pi)$. The $(0, 0)$ is a stable equilibrium, while the $(0, \pi)$ is stable in the ϕ -state regime ($UN = J < 1$) and

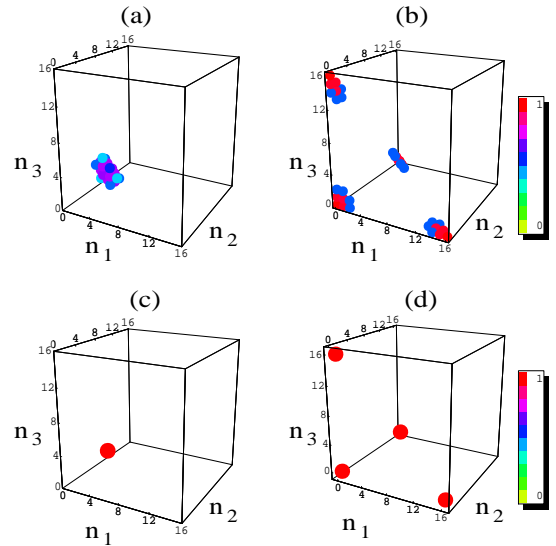


FIG. 4: Four well stationary and time evolved states: (a) ground state, (b) highest excited state, (c) phase engineered fragmented state following a $\pi/2$ relative phase shift of the ground state, (d) an entangled state evolved from the ground state following a $\pi/3$ relative phase shift. The three dimensions show the Fock state indices n_1, n_2 and n_3 , probabilities are shown in the color intensity scale. For graphical clarity, only the points higher than 40% of the highest probability are shown, with the highest probabilities normalized to 1.

unstable otherwise ($UN = J > 1$). Exploitation of the bifurcation characteristics of the unstable equilibrium generates entanglement. Taking the initial parameters such that there is an unstable hyperbolic fixed point, phase imprinting moves the ground state to the unstable point, and the wave packet splits in the subsequent time evolution. Control of the barrier height can then be used in three different ways to control the motion of the wave packet and thereby the nature of the desired entanglement [17]. First, a simultaneous ramping of the barrier with the natural dynamics at the unstable fixed point has been empirically found to be useful in directing the desired evolution of the wavepacket. Second, initial barrier height, that is the initial squeezing, helps shape the initial wave packet stretching it into different regions of accessible phase space; and, thirdly the initial barrier height sets the (negative) curvature of the potential at the hyperbolic fixed point, controlling the rate of splitting of the wave packet. All of these effects can be visualized for the double well system in the appropriate phase space [17]. Similar to the simple double well, the triple well, $M = 3$, can be thought of as two coupled pendulums [19] with complicated dynamics. In the (n, ϕ) representation, the unstable fixed points are $(0, 0, \frac{2k}{3}, \frac{2k}{3})$, $k = 1, 2$. All the features of the double well entanglement generation apply to the three well case, and thus, many of the insights from the two and three well dynamics can be extended to arbitrary number of wells in a circular array.

Next, we explore the dynamics of the $\frac{\pi}{2}$ and π phase shifting for the symmetric four well case. First we look at the ground and the highest excited state in Figs. 4 (a) and (b) for $N = 16, U = 0.25, J = e^{-1}, \phi = 0.175$, and assuming the case of ^{87}Rb in the previous example. As expected, the ground state is an approximate Gaussian and the highest state is an extreme entangled number state. The fixed point dynamics for the $\frac{\pi}{2}$ configuration is such that, for a constant barrier height, the state evolves into a number-squeezed state during its evolution towards an entangled state. Fig. 4 (c) shows a fragmented state (at 14 ms), with essentially exactly 4 particles in each well, obtained by this phase engineering scheme. Due to the location of the fixed points in the phase space, the entangled states generated by the $\frac{\pi}{2}$ imprinting are not as extreme or sharp as those generated by the π method; an example of the latter is shown in Fig. 4 (d) (at 1.5 ms). We also found that a $\frac{3}{2}$ phase difference between the wells produced entangled states that only differ by a symmetry from the $\frac{\pi}{2}$ phase imprinted states. Fragmented states have been observed in a 12 well optical lattice with adiabatic raising of the barrier [7]. We have shown here that fragmented states can also be created in a natural and efficient fashion without adiabatic constraints. In comparing our results to the results of Ref. [20], we show that the configuration in an even number of wells that they identified is a special case of many phase imprint dynamics that generate interesting correlated states in multiple wells. Their changes in system parameters is to drive the system from stability to a regime of instability. On the other hand, we take our system to be in the unstable regime and demonstrate the controllability of entangled states with barrier manipulation; potentially useful for experimental detection.

For the two, three, and four wells, we find $M - 1$ distinct phase differences between the neighboring wells for the multiwell fixed points [19, 21]. These are given by a general formula $\frac{2\pi j}{M}$ where $j = 1; 2; \dots; M - 1$, with M being the number of wells, which gives a π phase difference for the $M = 2$ double well, a $\frac{2\pi}{3}$ and $\frac{4\pi}{3}$ phase difference for the $M = 3$ triple well, and a $\frac{\pi}{2}$, π , and $\frac{3\pi}{2}$ phase difference for the $M = 4$ quadruple well configuration - we demonstrated the dynamics generated by all of these phase difference imprints. Note that the total change in phase in the circular loop is a multiple of 2π , a vortex like condition. We thus propose a general formula for M wells,

$$\phi_j = \frac{2\pi j}{M}, \quad (5)$$

for the constant phase offset between neighboring wells leading to the dynamical generation of entangled states. Here $j = 1; 2; \dots; M - 1$, and Eq. (5), being valid for any number of wells, even or odd, provides a substantial generalization of the phase offset mentioned in Ref. [20], which is valid only for the special cases of an even number

of wells and for $j = M - 2$ (phase offset). The multiplicity of Eq. (5) is prominent for large number of wells, e.g. for 12 wells, there are 11 phase offset possibilities. As in the three and four well case considered, symmetries may prevent all the imprinting offsets of Eq. (5) from generating independent dynamics.

In conclusion, we have demonstrated phase engineering schemes for the generation of entangled number states and fragmented states of BECs in multiple wells. By controlling the initial barrier height and rate of ramping, the entanglement of the final state can be tuned. We presented a novel series of formulae for the initial phase difference between the neighboring wells that is valid for any number of wells, even or odd, each having distinct properties. The creation, characterization, and applications of multidimensional/multipositional Schrodinger cat states of atoms remain largely unexplored experimentally, and the theoretical ramifications of such states, should they be easily produced, are just emerging.

This work was supported by NSF grant PHY-0140091 and DOE computational science graduate fellowship program grant DE-FG 02-97ER 25308.

Present address: Department of Physics, University of Michigan, Ann Arbor, MI 48109, USA

- [1] A. Einstein, B. Podolsky, and N. Rosen, Phys. Rev. 47, 777 (1935).
- [2] J. S. Bell, Speakable and Unsayable in Quantum Mechanics (Cambridge Univ. Press, Cambridge, 1987).
- [3] D. Bouwmeester et al., Phys. Rev. Lett. 82, 1345 (1999).
- [4] C. A. Sacket et al., Nature 404, 256 (2000).
- [5] O. Mandel et al., Nature 425, 937 (2003).
- [6] M. G. Reiner, O. Mandel, T. Esslinger, T. W. Hansch, and I. Bloch, Nature 415, 39 (2002).
- [7] C. Ozeel, A. K. Tuchman, M. L. Fensclau, M. Yasuda, and M. A. Kasevich, Science 291, 2386 (2001).
- [8] S. F. Huelga et al., Phys. Rev. Lett. 79, 3865 (1997); D. Jaksch et al., Phys. Rev. Lett. 82, 1975 (1999).
- [9] J. S. Bell, Physics 1, 195 (1965).
- [10] D. M. Greenberger, M. A. Home, A. Shimony, and A. Zeilinger, Am. J. Phys. 58, 1131 (1990).
- [11] N. J. Cerf, S. Massar, and S. Popescu, Phys. Rev. Lett. 89, 080402 (2002).
- [12] E. Schrodinger, Naturwissenschaften 23, 807 (1935).
- [13] J. R. Friedman et al., Nature 406, 43 (2000); C. H. van der Wal et al., Science 290, 773 (2000).
- [14] M. P. A. Fisher et al., Phys. Rev. B 40, 546 (1989); D. Jaksch et al., Phys. Rev. Lett 81, 3108 (1998).
- [15] A variety of array configurations have been studied, including linear and circular arrays. The trimeric linear array with dimering has been studied by: P. Buonsante, R. Franzosi, V. Penna, Phys. Rev. Lett 90, 050404 (2003). See also: L. Amico, A. Osterloh, and F. C. Cataliotti, cond-mat/0501648.
- [16] J. Denschlag et al., Science 287, 97 (2000); S. Burger et al., Phys. Rev. Lett. 83, 5198 (1999).
- [17] K. W. Mahmud, H. Perry, and W. P. Reinhardt, J.

- Phys. B 36, L265 (2003); K. W. M. Ahmed, H. Perry, and W. P. Reinhardt, Phys. Rev. A 71, 023615 (2005).
- [18] A. Smerzi, S. Fantoni, S. Giovanazzi, and S. R. Shenoy, Phys. Rev. Lett. 79, 4950 (1997); S. Raghavan et al., 59, 620 (1999).
- [19] R. Franzosi and V. Penna, Phys. Rev. E 67, 046227 (2003).
- [20] A. Polkovnikov, Phys. Rev. A 68, 033609 (2003); A. Polkovnikov et al., Phys. Rev. A 66, 053607 (2002).
- [21] L. Casetti and V. Penna, J. Low T Phys 126, 455 (2002).